

1 **SUPPLEMENTARY MATERIALS**

2 **Targeting WWP1 ameliorates cardiac ischemic injury by suppressing KLF15-ubiquitination**  
3 **mediated myocardial inflammation**

4  
5 Xia Lu<sup>1#</sup>, Boshen Yang<sup>1#</sup>, Ruiqiang Qi<sup>2</sup>, Qifei Xie<sup>2</sup>, Taixi Li<sup>1</sup>, Jie Yang<sup>3</sup>, Tingting Tong<sup>3</sup>, Kaifan Niu<sup>1</sup>,  
6 mingyu Li<sup>4</sup>, Weijun Pan<sup>5</sup>, Yongxin Zhang<sup>6</sup>, Dongmei Shi<sup>1</sup>, Suiji Li<sup>2</sup>, Cuilian Dai<sup>2</sup>, Chengxing Shen<sup>1</sup>,  
7 Xiaoqing Wang<sup>1\*</sup>, Yan Wang<sup>2\*</sup> and Juan Song<sup>2\*</sup>

8  
9 <sup>1</sup>Department of Cardiology, Shanghai Sixth People's Hospital Affiliated to Shanghai Jiao Tong University  
10 School of Medicine, Shanghai 200233, China.

11 <sup>2</sup> Xiamen Cardiovascular Hospital, Xiamen University, Xiamen 361004, China.

12 <sup>3</sup> Key Laboratory of Targeted Intervention of Cardiovascular Disease, Collaborative Innovation Center  
13 for Cardiovascular Disease Translational Medicine, Nanjing Medical University, Nanjing 211166,  
14 Jiangsu, China.

15 <sup>4</sup>Fujian Provincial Key Laboratory of Innovative Drug Target Research, School of Pharmaceutical  
16 Sciences, Xiamen University, Xiamen 361102, China.

17 <sup>5</sup>Key Laboratory of Tissue Microenvironment and Tumor, CAS Center for Excellence in Molecular Cell  
18 Science, Shanghai Institute of Nutrition and Health, Shanghai Institutes for Biological Sciences,  
19 University of Chinese Academy of Sciences, Chinese Academy of Sciences (CAS), Shanghai, China.

20 <sup>6</sup> The first clinical medical college, Southern Medical University, Guangzhou 510000, China.

21 \*Corresponding authors:

22 Juan Song: [songjuan\\_ok@163.com](mailto:songjuan_ok@163.com)

23 Yan Wang: [wy@medmail.com.cn](mailto:wy@medmail.com.cn)

24 Xiaoqing Wang: [xq\\_w@outlook.com](mailto:xq_w@outlook.com)

25 #These authors contributed equally to this work.

31 **MATERIALS AND METHODS**

32 **Echocardiography**

33 Cardiac functions were evaluated by echocardiography (GE Vivid 7 equipped with a 14-MHz phase array  
34 linear transducer, S12, allowing a 150 maximal sweep rate) in Figure 2, Figure 8, Figure 11, and Figure  
35 S5. Cardiac functions were tested with a high-resolution ultrasound imaging system (MyLab Touch:  
36 Esaote, Italy linear array probe, frequency 18-22 MHz) in Figure 7. All measurements were performed  
37 by an observer blinded to the identities of the tracings and averaged over five consecutive cardiac cycles.  
38 Left ventricle (LV) end diastolic volume (LVEDV) and LV end systolic volume (LVESV) were calculated  
39 using the biplane area-length method. LV ejection fraction (EF%) was calculated following the formula:  
40  $EF\% = [(LVEDV-LVESV)/LVEDV] \times 100\%$ . The 2D-guided left ventricular M mode tracings at the  
41 papillary muscle level were recorded from the long-axis view to measure LV internal diameter at end  
42 systole (LVIDs) and at end diastole (LVIDd). LV fractional shortening (FS%) was calculated according  
43 to the following formula:  $FS\% = [(LVIDd-LVIDs)/LVIDd] \times 100\%$ . The representative image of each  
44 group was selected based upon the mean value.

45 **Cell culture**

46 Neonatal rat cardiac myocytes (NRCMs) were isolated from 1 to 3-day-old neonatal Sprague-Dawley  
47 rats (Beijing Vital River Laboratory Animal Technology Co., Ltd.). NRCMs were plated at a density of  
48  $1 \times 10^6$  cells/ml and cultured in Dulbecco's Modified Eagle Medium (DMEM, Invitrogen Corporation,  
49 USA), supplemented with penicillin, streptomycin, and 10% FBS. The cells were put on serum-free  
50 medium and subsequently infected with Adv-GFP (MOI = 50) or Adv-WWP1 (MOI = 50) for 4 h, and  
51 then the medium containing the adenovirus was removed and replaced by DMEM supplemented with  
52 10% FBS. After 48 h of infection, NRCMs cultured in serum-free and glucose deprived DMEM under  
53 hypoxia for 6 h induced by a hypoxia chamber (Thermo, HERA cell 150i) with 5% CO<sub>2</sub>, 1% O<sub>2</sub>, and 94%  
54 N<sub>2</sub>. NRCMs cultured in serum-free medium and normoxia with 5% CO<sub>2</sub> acted as controls. H9C2 cells  
55 and RAW264 cells purchased from Cell Bank of the Chinese Academy of Sciences (Shanghai, China)  
56 were cultured in DMEM supplemented with 10% FBS, penicillin and streptomycin. H9C2 cells were  
57 seeded into 96-well plates. Cell Counting Kit-8 (CCK-8) (DOJINDO, Japan, Cat#AY-4710P) were used  
58 to analysis the cell viability according to the instruction.

59 **Western blot**

60 Briefly, Western blot analyses were performed using commercially available antibodies: anti-WWP1  
61 (ab43791, abcam, 1:1000), anti-KLF15 (sc-271675, Santa Cruz, 1:100), anti-Ub K48 (12805S, abcam,  
62 1:1000), anti-Bcl2 (15071S, SCT, 1:1000), anti-Bax (5023S, CST, 1:1000), anti-Cleaved-caspase 3  
63 (9661S, CST, 1:1000), anti-p65 (AF1234, Beyotime, 1:1000), anti-p300 (86377S, CST, 1:1000), anti-  
64 AcK310 (19870, abcam, 1:1000), anti-P38 (AF1111, Beyotime, 1:1000), anti-ERK1/2 (AF1051,  
65 Beyotime, 1:1000), anti-p-ERK1/2 (AF1891, Beyotime, 1:1000), anti-GAPDH (HRP60004, Proteintech,  
66 1:10000), anti-Tubulin (AF7819-1, Beyotime, 1:1000), anti-LaminB1 (AF1408, Beyotime, 1:1000), anti-  
67 CD68 (A6554, Abclonal, 1:1000), anti-Ly6G (A20861, Abclonal, 1:1000), anti-Flag (AF519-1,  
68 Beyotime, 1:1000), anti-HA (AF5057, Beyotime, 1:1000) followed by incubation with peroxidase-  
69 conjugated secondary antibodies. The signals were detected with the enhanced-chemiluminescent (ECL)  
70 system (Tanon, China) and quantified by scanning densitometry with the Image J software. GAPDH and  
71 Lamin B1 served as the loading control. The results from each experimental group were expressed as  
72 relative integrated intensity compared with the control group measured at the same time.

73 **Real-time PCR**

74 Table S1. Primer sequences.

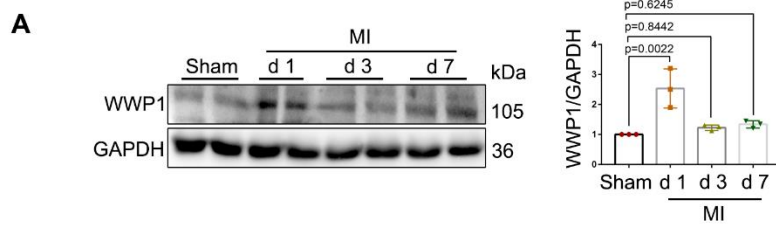
Genes	Primer sequences	
Mus HPRT	Forward	GTTGGATACAGGCCAGACTTTGT
	Reverse	GATTCAACTTGCCTCATCTTAGGC
Mus IL-6	Forward	CCGGAGAGGAGACTTCACAG
	Reverse	TCCACGATTCCCAGAGAAC
Mus IL-1 $\beta$	Forward	GCAACTGTTCTGAACTCAACT
	Reverse	ATCTTTGGGGTCCGTCAACT
Mus VCAM-1	Forward	GAACCCAAACAGAGGCAGAG
	Reverse	GGTATC CCATCACTTGAGCAG
Mus MCP-1	Forward	TAGCATCCACGTGCTGTCTC

	Reverse	CAGCCGACTCATTGGGATCA
Rat HPRT	Forward	GCTGAAGATTTGGAAAAGGTGT
	Reverse	ACAGAGGGCCACAATGTGAT
Rat IL-6	Forward	ACCAGAGGAAATTTTCAATAGGC
	Reverse	TGATGCACTTGCAGAAAACA
Rat IL-1 $\beta$	Forward	GGTCAAAGGTTTGGGAAGCAG
	Reverse	TGTGAAATGCCACCTTTTGA
Rat TNF- $\alpha$	Forward	AGGGTCTGGGCCATAGAACT
	Reverse	CCACCACGCTCTTCTGTCTAC

---

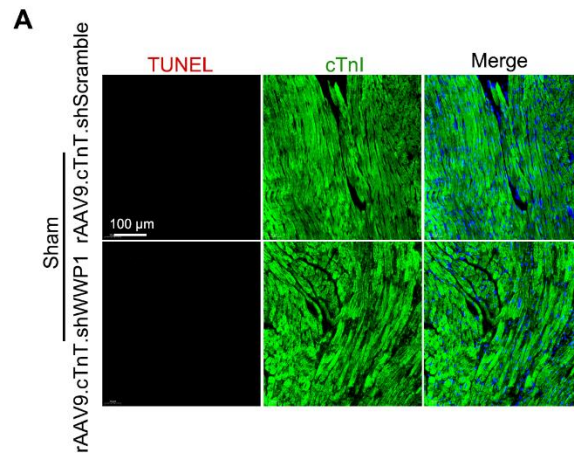
75 **TUNEL assay**

76 The heart tissues were embedded in paraffin, cut at 8  $\mu$ m, dewaxed and rehydrated, and then  
77 permeabilized with 20  $\mu$ g/mL proteinase K for 10 min. The staining was performed using an In Situ Cell  
78 Death Detection Kit (12156792910, Roche) according to the protocol. Positive controls were  
79 administered with DNase I, while TdT was omitted from the reaction process to provide negative controls.  
80 The percentage of apoptotic cardiomyocytes was calculated as TUNEL-positive nuclei number with  
81 simultaneous cTnI-positive staining divided by the total number of cTnI-positive stained cells. Five  
82 random fields of vision were photographed with a confocal microscope (Zeiss, German). For cultured  
83 cells, NRCMs were fixed with formaldehyde for 15 min on ice and washed with PBS. NRCMs were  
84 permeabilized with 0.3% Triton X-100 for 5 min. TUNEL detection solution was added and incubated  
85 with NRCMs at 37  $^{\circ}$ C for 60 min away from light. NRCMs were washed with PBS and stained with  
86 DAPI sequentially. Then, five fields were randomly selected to take pictures in each group with  
87 fluorescence microscope (OLYMPUS TH4-200, Japan). TUNEL-positive nuclei numbers were  
88 quantified by Image J software.



90

91 **Figure S1. WWP1 expression peaks on the first day post-MI.** A Mice hearts subjected to LAD ligation  
 92 were harvested at day 1, 3, and 7, respectively. Representative Western blot was performed to detect the  
 93 temporal protein expression pattern of WWP1 in the infarct area (infarct and border zone), and statistical  
 94 result was shown. n = 3. The data are shown as the means  $\pm$  SD. The data shown was analysed by  
 95 unpaired Student's t-test.



96

97 **Figure S2. Cardiomyocyte-specific overexpressing WWP1 does not affect the apoptosis of**

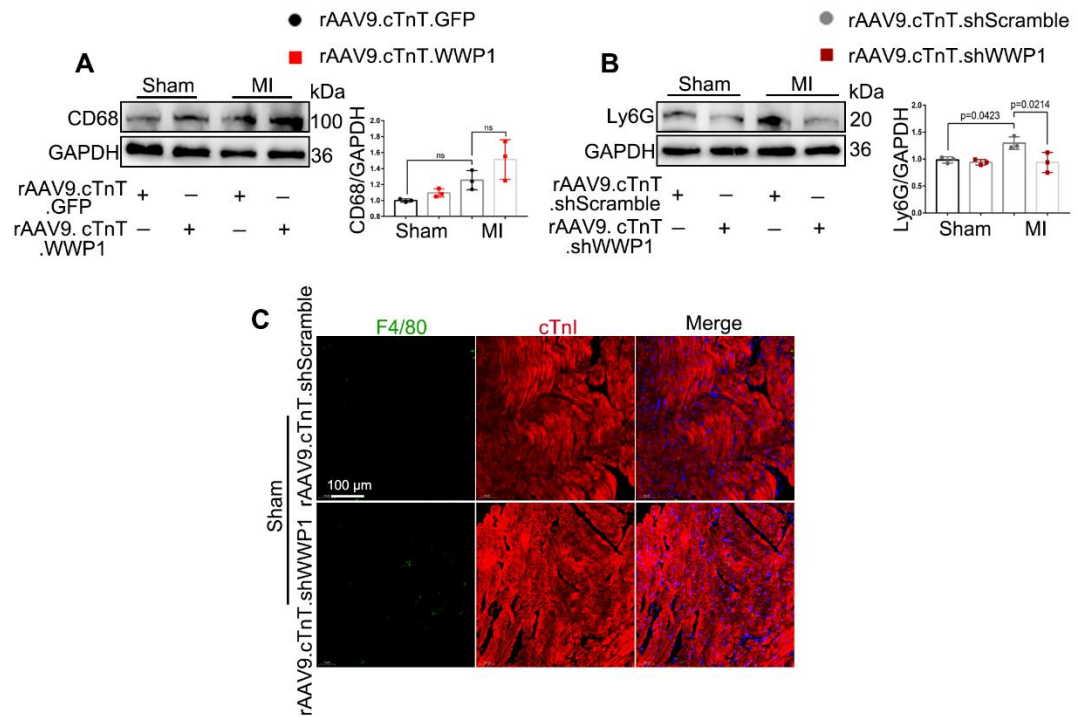
98 **cardiomyocytes in sham-mice hearts. A** Mice were treated with rAAV9-cTnT-shScramble or rAAV9-

99 cTnT-shWWP1 by intravenous injection of tail two weeks before suffering from sham or LAD ligation,

100 and after additional 3 days, mice were sacrificed. TUNEL assay and immunofluorescence staining with

101 cTnI were performed to detect cardiomyocyte apoptosis in the myocardium. Scale bar = 100  $\mu\text{m}$ . n = 3.

102



103

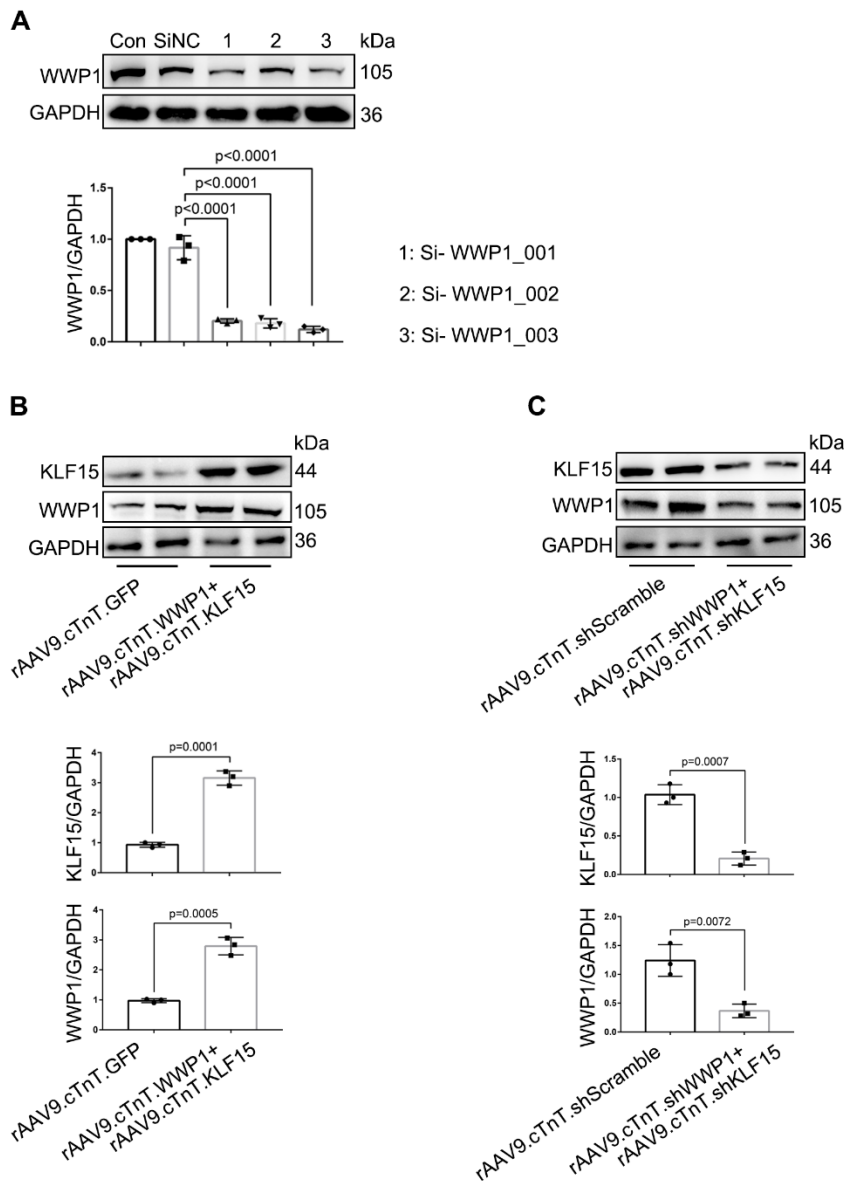
104 **Figure S3. WWP1 affects the inflammation of cardiomyocytes at early phase post-MI. A, B**

105 Representative Western blots were performed to detect the CD68 and Ly6G expression in the infarct area,

106 and statistical results were shown. n = 3. C Immunofluorescence co-staining for cTnI with F4/80 and

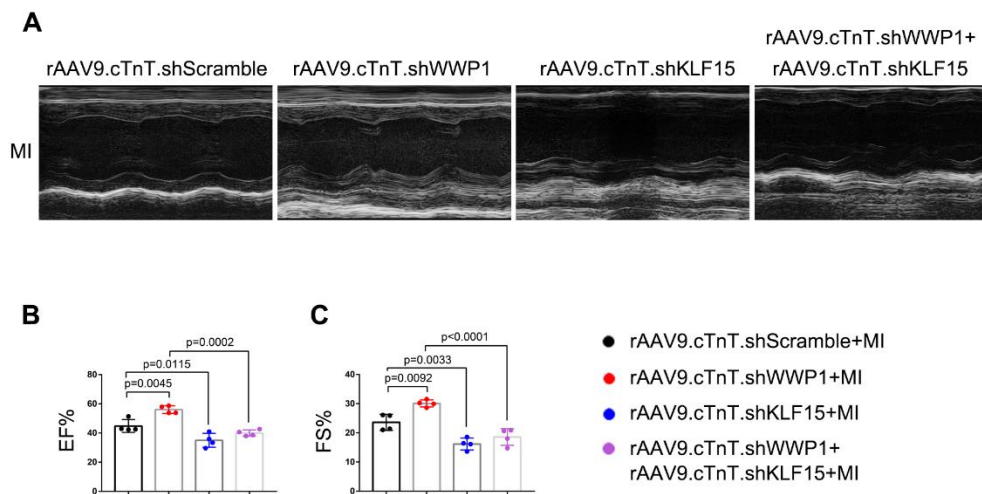
107 DAPI in infarcted hearts. Scale bar = 100  $\mu$ m. n = 3. The data are shown as the means  $\pm$  SD. The data

108 shown in **A**, and **B** were analysed by one-way ANOVA followed by Bonferroni post hoc test.



109

110 **Figure S4. The protein expression of WWP1.** A H9C2 cells were transfected with Si-WWP1 for 36 h,  
 111 and representative Western blot was performed to test the protein change of WWP1. n = 3. **B** Mice were  
 112 injected with rAAV9-cTnT-WWP1 with or without rAAV9-cTnT-KLF15 for two weeks, and  
 113 representative Western blot was performed to test the protein change of WWP1 in mice hearts. n = 3. **C**  
 114 Mice were injected with rAAV9-cTnT-shWWP1 with or without rAAV9-cTnT-shKLF15 for two weeks,  
 115 and representative Western blot was performed to test the protein change of WWP1 in mice hearts. n =  
 116 3. The data are shown as the means  $\pm$  SD. The data shown in **A** was analysed by one-way ANOVA  
 117 followed by Bonferroni post hoc test, and shown in **B**, and **C** were analysed by unpaired Student's t-test.



118

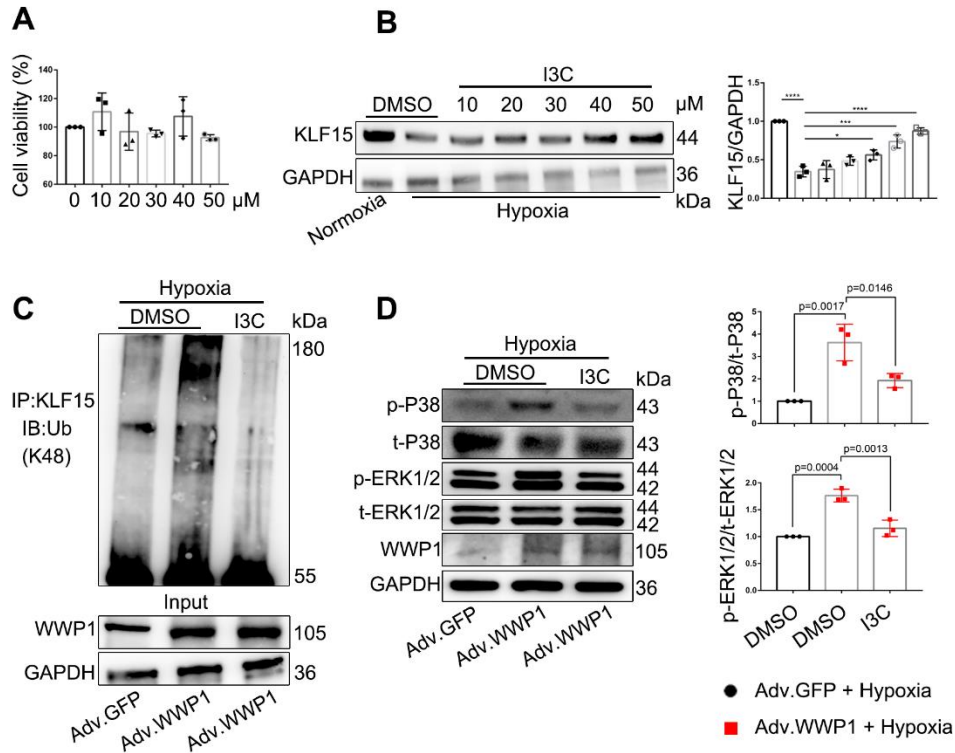
119 **Figure S5. The regulatory role of WWP1 on cardiac function post-MI is dependent on KLF15.**

120 Mice were injected with rAAV9-cTnT-shWWP1 with or without rAAV9-cTnT-shKLF15 before they

121 subjected to MI. **A-C** Cardiac function were measured by echocardiography at day 3 post-MI. n = 4. The

122 data are shown as the means  $\pm$  SD. The data shown in **B**, and **C** were analysed by one-way ANOVA

123 followed by Bonferroni post hoc test.



124

125 **Figure S6. I3C treatment suppresses KLF15-degradation mediated activation signals in hypoxia-**

126 **induced H9C2 cells. A** H9C2 cells were infected with Adv-WWP1 or Adv-GFP for 24 h followed by

127 I3C (50 μM) treatment for 24 h, and then the cells were treated with hypoxia for 6 h. CCK8 was applied

128 to detect the viability of H9C2 cells treated with different concentration of I3C. n = 3. **B** Representative

129 Western blot was performed to test the protein change of KLF15 in hypoxia-induced H9C2 cells treated

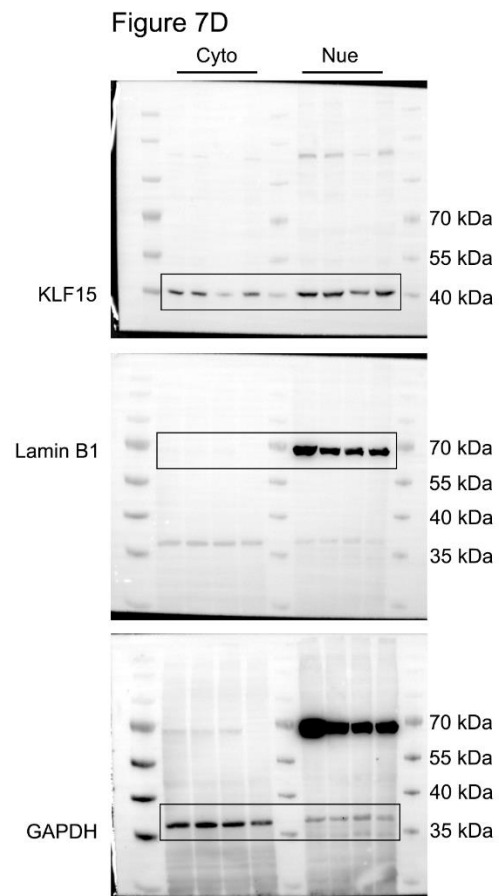
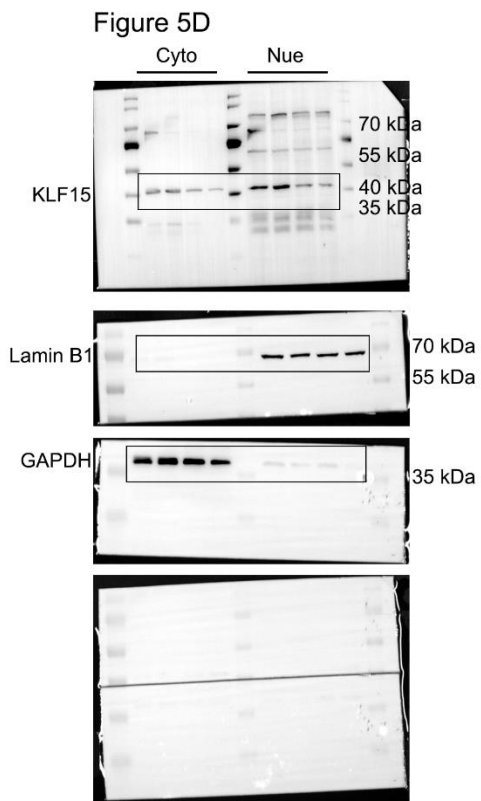
130 with different concentration of I3C. n = 3. **C** Cellular proteins were isolated for immunoprecipitation

131 with anti-KLF15 antibody followed by immunoblot with anti-Ub-K48 antibody. n = 3. **D** Levels of

132 phosphorylated P38 and ERK1/2 were examined by Western blots, and statistical results were shown. n

133 = 3. The data are shown as the means ± SD. The data shown in **A**, **B**, and **D** were analysed by one-way

134 ANOVA followed by Bonferroni post hoc test.



135

136 **Figure S7.** Images of Western blot without cutting.